Opening angles, Lorentz factors and confinement of X-ray binary jets

J. C. A. Miller-Jones,[1][*] R. P. Fender[2] and E. Nakar[3]

[1]*Astronomical Institute 'Anton Pannekoek', University of Amsterdam, Kruislaan 403, 1098 SJ Amsterdam, the Netherlands*
[2]*School of Physics and Astronomy, University of Southampton, Highfield, Southampton SO17 1BJ*
[3]*Theoretical Astrophysics, Caltech, Pasadena, CA 91125, USA*

ABSTRACT

We present a collation of the available data on the opening angles of jets in X-ray binaries, which in most cases are small ($\lesssim 10°$). Under the assumption of no confinement, we calculate the Lorentz factors required to produce such small opening angles via the transverse relativistic Doppler effect. The derived Lorentz factors, which are in most cases lower limits, are found to be large, with a mean >10, comparable to those estimated for active galactic nuclei (AGN) and much higher than the commonly assumed values for X-ray binaries of 2–5. Jet power constraints do not, in most cases, rule out such high Lorentz factors. The upper limits on the opening angles show no evidence for smaller Lorentz factors in the steady jets of Cygnus X-1 and GRS 1915+105. In those sources in which deceleration has been observed (notably XTE J1550−564 and Cygnus X-3), some confinement of the jets must be occurring, and we briefly discuss possible confinement mechanisms. It is however possible that all the jets could be confined, in which case the requirement for high bulk Lorentz factors can be relaxed.

Key words: relativity – stars: winds, outflows – ISM: jets and outflows – X-rays: binaries.

1 INTRODUCTION

Proper motions of X-ray binary (XRB) jets have often been used to place limits on the jet Lorentz factors. Fender (2003) recently argued that it was in fact impossible to do more than place a lower limit on the Lorentz factors of the jets from two-sided jet proper motions. For the persistent, continuous jets observed to exist in the low/hard X-ray states of black hole candidates, Gallo, Fender & Pooley (2003) found a universal correlation between the X-ray and radio fluxes of the sources, and used the scatter about this relation to constrain the Lorentz factors of such jets to $\lesssim 2$. However, Heinz & Merloni (2004) argued that the scatter about such a relation could not be used to constrain the mean Lorentz factor of the jets, but rather only the width of the Lorentz factor distribution. Other arguments, such as those based on jet power requirements, must be used to determine the absolute values of the jet Lorentz factors.

Bulk jet flow velocities close to c, the speed of light, have been inferred in many XRB systems (e.g. Mirabel & Rodríguez 1994; Hjellming & Rupen 1995; Fender et al. 2004b), whereas the transverse expansion speeds have not yet been reliably measured. To date, there are few reported detections of XRB jets resolved perpendicular to the jet axis. This places strong upper limits on the opening angles of the jets (often less than a few degrees; see Table 1), and hence on the transverse expansion speeds. While jets can in principle undergo transverse expansion at a significant fraction of c,

time dilation effects associated with the bulk motion would reduce the apparent opening angle in the observer's frame. The magnitude of this effect would be determined by the bulk Lorentz factor of the flow. This raises the possibility of using the observed opening angle of a freely expanding jet to constrain its Lorentz factor. Alternatively, if the Lorentz factors thus derived were incompatible with values deduced from independent methods, a strong argument could be made for jet confinement out to large (parsec) scales in such Galactic sources.

In this paper, we first develop the formalism for deducing the Lorentz factor of a freely expanding jet given a measurement of the opening angle and the inclination angle of the jet axis to the line of sight. In Section 3, we compare constraints on the Lorentz factors derived from opening angle considerations with those from other methods. Transient and steady jets are compared in Section 4, and the derived XRB jet Lorentz factors are compared to those seen in active galactic nuclei (AGN) in Section 5. We discuss possible mechanisms for jet confinement and a method of using light curves to test confinement in Section 6. A summary of the observed properties of the individual sources is given in Appendix A.

2 FORMALISM

We consider the case of knots (although we note that they could be internal shocks rather than plasmons) propagating in an XRB jet. To simplify matters, we consider a single, spherical knot expanding radially with constant velocity $u' = \mathrm{d}r'/\mathrm{d}t'$ in its own frame. Primed quantities are measured in the frame of the moving knot and

[*]E-mail: jmiller@science.uva.nl

Table 1. Summary of the observations from the literature. $\Gamma_{\mathrm{min,exp}}$ denotes the Lorentz factors derived from the opening angles (equation 4) and the constraints on $\beta \cos i$, and Γ_{d} the Lorentz factors derived from the ratio d/d_{max} (equation 10). The first column of references gives the papers from which the values of ϕ, $\beta \cos i$ and d_{max} were derived. The second gives the papers from which the distance estimates were taken. D00b = Dhawan et al. (2000b); D00 = Dhawan, Goss & Rodríguez (2000a); F99 = Fender et al. (1999); MJ04 = Miller-Jones et al. (2004); D83 = Dickey (1983); M01 = Martí et al. (2001); HR95 = Hjellming & Rupen (1995); H00 = Hjellming et al. (2000); O01 = Orosz et al. (2001); P02 = Paredes et al. (2002a); R02a = Ribó et al. (2002a); T03 = Tomsick et al. (2003); O02 = Orosz et al. (2002); C05 = Corbel et al. (2005); S01 = Stirling et al. (2001); M95 = Massey, Johnson & Degioia-Eastwood (1995); F06 = Fender et al. (2006); G04 = Gallo et al. (2004); H04 = Hynes et al. (2004); R02b = Ribó et al. (2002b).

System	ϕ	$\beta \cos i$	$\Gamma_{\mathrm{min,exp}}$	d_{max}(kpc)	Reference	d (kpc)	Reference	Γ_{d}
GRS 1915+105 (steady)	$\leqslant 4.9°$	0.035 ± 0.017	11.7		D00b	6.1–12.2	D00	
GRS 1915+105 (transient)	$\leqslant 4°$	0.41 ± 0.02	15.7	11.2 ± 0.8	F99	6.1–12.2	D00	>1.8
Cygnus X-3 (small scale)	$5.0 \pm 0.5°$	0.50 ± 0.10	13.3	35.7 ± 4.8	MJ04	~ 10	D83	1.2 ± 0.1
Cygnus X-3 (large scale)	$<16.5°$	0.14 ± 0.03	3.6	21 ± 1	M01	~ 10	D83	1.2 ± 0.1
GRO J1655−40	$\lesssim 3.1°$	0.091 ± 0.014	18.6	3.5 ± 0.1	HR95	3.2 ± 0.2	HR95	>2.4
V4641 Sgr	$\leqslant 25.1°$	~ 0.4	2.6		H00	$9.59^{+2.72}_{-2.19}$	O01	
LS 5039	$\leqslant 6°$	0.17 ± 0.05	9.7		P02	2.9 ± 0.3	R02a	
XTE J1550−564	$\leqslant 3.7°$	0.61 ± 0.13	19.6	16.5 ± 3.5	T03	3.2–9.8	O02	1.3 ± 0.2
H 1743−322	$\leqslant 6°$	0.23 ± 0.05	9.8	10.4 ± 2.9	C05	$8.5?$		
Cygnus X-1 (steady)	$<2°$	>0.50	33.0		S01	2.1 ± 0.1	M95	
Cygnus X-1 (transient)	$<18°$	>0.2	3.7		F06	2.1 ± 0.1	M95	
GX 339−4	$\leqslant 12°$	$>0.16 \pm 0.05$	4.9		G04	>6	H04	
1RXS J001442.2+580201	$\leqslant 1.8°$	0.20 ± 0.02	32.5		R02b			

unprimed quantities in the frame of the stationary observer. The expansion speed of the knot as seen in the observer's frame is modified by the relativistic Doppler factor, and is thus

$$u = \frac{u'}{\Gamma(1 - \beta \cos i)} = \delta u', \qquad (1)$$

where $\delta = \Gamma^{-1}(1 - \beta \cos i)^{-1}$ is the Doppler factor, βc is the jet speed, $\Gamma = (1 - \beta^2)^{-1/2}$ is the bulk Lorentz factor of the jet and i is the inclination angle of the jet axis to the line of sight. The geometry is shown in Fig. 1.

In most cases, we do not observe the actual expansion velocity directly. Most of the observations simply place a constraint on the half-opening angle ϕ of the jet from its width at a given distance from the core. The observed knot radius at a given time t (in the observer's frame) since the knot was ejected is $r = ut$. The apparent speed of the knot away from the core is $\beta_{\mathrm{app}} c$ given by

$$\beta_{\mathrm{app}} = \frac{\beta \sin i}{1 - \beta \cos i}, \qquad (2)$$

having taken into account the combination of projection effects and the motion of the knot towards the observer. Thus, since the observed distance of the knot from the core is $R = \beta_{\mathrm{app}} ct$, then

$$\tan \phi = \frac{r}{R} = \frac{u'}{\Gamma \beta c \sin i}. \qquad (3)$$

Rearranging, we can therefore derive an expression for the bulk jet Lorentz factor implied by the measured opening angles, writing the intrinsic jet knot expansion speed as $u' = \beta_{\mathrm{exp}} c$. Thus

$$\Gamma = \left(1 + \frac{\beta_{\mathrm{exp}}^2}{\tan^2 \phi \sin^2 i}\right)^{1/2}. \qquad (4)$$

Whereas i alone is difficult to constrain, in many cases $\beta \cos i$ is a measurable variable. Knowing ϕ, we can then find Γ as a function of i, from $i = 0$ up to $i_{\mathrm{max}} = \cos^{-1}(\beta \cos i)$. This can then be compared at each value of i to the value of $\Gamma = (1 - \beta^2)^{-1/2}$ obtained from $\beta \cos i$.

β_{exp} is commonly assumed to have an upper limit corresponding to the relativistic sound speed, $c/\sqrt{3}$. However, the acceleration of

a cloud of hot jet plasma that expands under its own pressure in a zero-pressure external medium without any confinement is not done by a sound wave, so the expansion velocity is limited by the initial thermal velocity and not by the sound velocity (Landau & Lifshitz 1959). Thus a jet that is initially relativistically hot can in principle undergo transverse expansion at the speed of light (e.g. Sari, Piran & Halpern 1999). We therefore performed our calculations up to the limit $\beta_{\mathrm{exp}} = 1$.

3 CONSTRAINTS ON THE LORENTZ FACTORS

3.1 Observational sample

We have amassed from the literature a compilation of the known X-ray binaries with resolved radio jets. A description of the individual systems is given in Appendix A. In most cases, the jets are unresolved perpendicular to the jet axis, giving an upper limit to the opening angle of the jets as observed in our frame, determined by the beam size and the angular separation from the centre of the system.

In those sources for which the proper motions of both the approaching and receding jet knots, μ_{a} and μ_{r}, respectively, can be measured, the product

$$\beta \cos i = \frac{\mu_{\mathrm{a}} - \mu_{\mathrm{r}}}{\mu_{\mathrm{a}} + \mu_{\mathrm{r}}}, \qquad (5)$$

may be calculated, constraining the values of $\beta > \beta \cos i$ and $i < \cos^{-1}(\beta \cos i)$. For a given source distance d, it is possible to solve for the exact values of β and i. There is therefore a maximum possible distance to the source,

$$d_{\mathrm{max}} = \frac{c}{\sqrt{\mu_{\mathrm{a}} \mu_{\mathrm{r}}}}, \qquad (6)$$

which corresponds to the maximum possible intrinsic jet speed, $\beta = 1$.
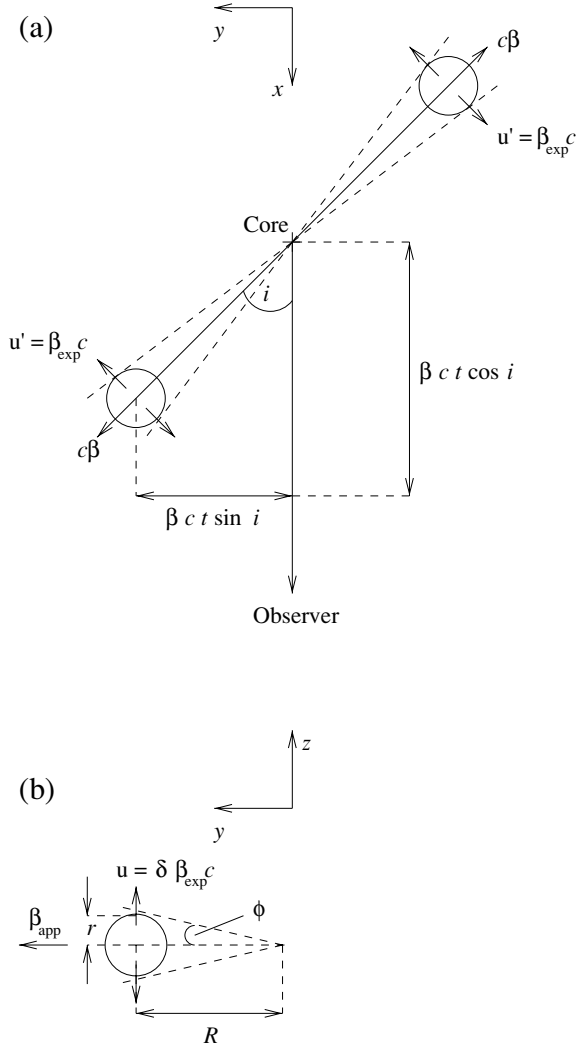
(a)

(b)

Figure 1. Schematic of the geometry of the jets. (a) Shows the plane of the knot motion, and (b) shows the motion as seen by the observer.

3.2 Lorentz factors from opening angle constraints

Plots of the Lorentz factors calculated from equation (4), assuming free expansion at c (i.e. $\beta_{exp} = 1$) in the source frame, are shown in Fig. 2 for the XRBs listed in Appendix A, along with the Lorentz factors derived from the constraints on $\beta \cos i$ given in Table 1. Since equation (4) contains four variables, then for $\beta_{exp} = 1$ and ϕ fixed at the value in Table 1, then with the constraint on $\beta \cos i$, there is a unique solution for Γ and i for each source. This is the point at which the solid and dashed lines meet in Fig. 2. We denote this value of Γ as $\Gamma_{min,exp}$, which is listed in Table 1. We note that the plotted values of Γ in Fig. 2 are all strictly lower limits calculated for a freely expanding source ($\beta_{exp} = 1$), since none of the jets (with the possible exception of Cygnus X-3) were resolved perpendicular to the jet axis, so we have only upper limits on the opening angles of the jets. From the figure, it is clear that the opening angles predict much higher Lorentz factors (with a mean of 13.7) than are permitted by the measurements of $\beta \cos i$, unless the source distances are all at or very close to d_{max}, the distance at which $i = i_{max}$ and $\beta = 1$. For the sources which are not very close to d_{max} (see Table 1 and Section 3.4), then the expansion speed must be less than c, i.e. *the jets are confined*.

If the jets are not freely expanding, but rather expand at some lower velocity, $\beta_{exp}c$, in their rest frame, then the jet Lorentz factors implied by the measured opening angles are lower. We can rearrange equation (4) as

$$\beta_{exp} = \tan\phi\{\Gamma^2[1 - (\beta\cos i)^2] - 1\}^{1/2}, \tag{7}$$

where, since $\beta > \beta\cos i$ as explained in Section 3.1, then we require $\Gamma > [1 - (\beta\cos i)^2]^{-1/2}$. Using the constraints on ϕ and $\beta\cos i$ in Table 1, we have plotted the predicted values of β_{exp} for different values of Γ in Fig. 3. This shows that only four of the jets have Lorentz factors $\Gamma < 5$ for $\beta_{exp} = 1$, as also seen in Table 1. If the Lorentz factors in XRB jets are all to lie within the commonly assumed range of $2 < \Gamma < 5$, then from Fig. 3, we can quantify the degree of confinement required. In that case, the jets with the highest derived Lorentz factors $\Gamma_{min,exp}$ have a maximum possible expansion speed of $\beta_{exp} \lesssim 0.15$. If the opening angles are indeed smaller than the upper limits quoted in Table 1, then this value would decrease further.

3.3 Lorentz factors from jet power constraints

The high bulk Lorentz factors derived from equation (4) would appear to imply high kinetic powers for the jets. Nine of the 13 jets listed in Table 1 have predicted $\Gamma_{min,exp} > 9$. Minimum energy requirements (e.g. Longair 1994), assuming that the source volume can be derived by equating the light crossing time of the source to the rise time of an outburst, give a minimum jet power of

$$P_{min}(\Gamma = 1) = 3.5 \times 10^{33} \eta^{4/7} \left(\frac{\Delta t}{s}\right)^{2/7} \left(\frac{d}{kpc}\right)^{8/7} \left(\frac{\nu}{GHz}\right)^{2/7}$$

$$\times \left(\frac{S_\nu}{mJy}\right)^{4/7} \quad erg\,s^{-1}, \tag{8}$$

where the source rise time Δt, the flux density S_ν and the frequency ν should be measured in the source rest frame, equivalent to the observer's frame for $\Gamma = 1$. η is the ratio of energy in relativistic electrons to the total energy. Since $\nu = \delta\nu'$, $S_\nu = \delta^{3-\alpha} S'_\nu$ (for a spectrum $S_\nu \propto \nu^\alpha$) and $\Delta t = \delta^{-1}\Delta t'$, then if $\Gamma \neq 1$, the two frames are no longer equivalent, and the correction,

$$P_{min}(\Gamma \neq 1) = \delta^{-4(3-\alpha)/7} P_{min}(\Gamma = 1), \tag{9}$$

is required if the measured values in the observer's frame are to be used. In all the sources considered, $\delta < 1$, such that increasing Γ implies an increase in the intrinsic source luminosity.

Fender, Belloni & Gallo (2004a) tabulate measured values of d, $M/M_\odot$ (where M is the mass of the compact object), Δt and $S_{5\,GHz}$ for several sources, allowing us to calculate for each of the sources the minimum power implied for the jets by the derived values of $\Gamma_{min,exp}$. This can be compared with the Eddington limiting luminosity, $L_{Edd} = 1.3 \times 10^{38} (M/M_\odot)$ erg s^{-1}, shown as the ratio P_{min}/L_{Edd} in Table 2. The values shown for Cygnus X-3 have been taken from Miller-Jones et al. (2004), and those shown for the 2001 flare of GRS 1915+105 ($\phi = 18.3° \pm 3.6°$) from Miller-Jones et al. (2005), to give an illustration of how variable flare power can be.

It is plausible that XRBs can exceed the Eddington limiting luminosity for a short time during outburst by a small factor. Thus, the Lorentz factors implied by the measured opening angle constraints are clearly ruled out by the total power requirement only in the case of Cygnus X-3, a source which we believe for other reasons to be confined (Section 3.5). Thus, in most cases, jet power constraints cannot rule out high Lorentz factors.
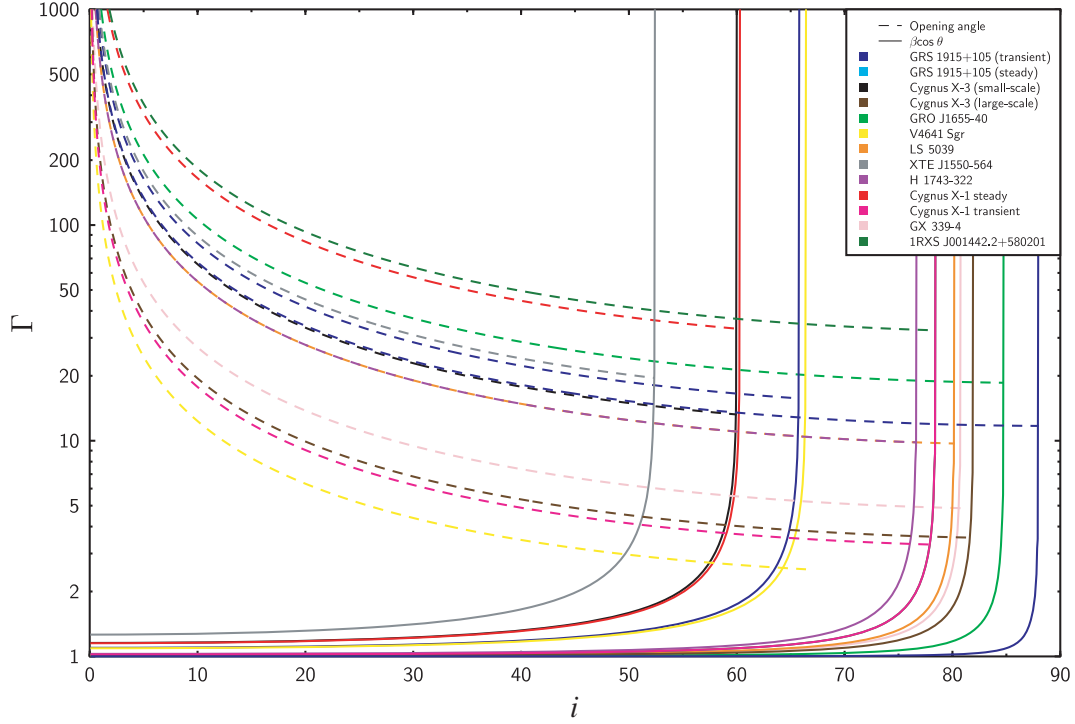
Figure 2. Lorentz factors derived from opening angle considerations (equation 4; dashed lines) and from $\beta \cos i$ (Table 1; solid lines) for a selection of Galactic XRBs. Since the opening angles given in Table 1 are upper limits, the Lorentz factors derived from them (the dashed lines) are in fact lower limits, assuming freely expanding jets with an expansion speed c. The Lorentz factor $\Gamma_{\mathrm{min,exp}}$ is defined as the Lorentz factor where the dashed and solid lines cross, i.e. the solution for Γ and i satisfying both equation (4) (for $\beta_{\mathrm{exp}} = 1$ and ϕ as listed in Table 1) and the constraint on $\beta \cos i$.
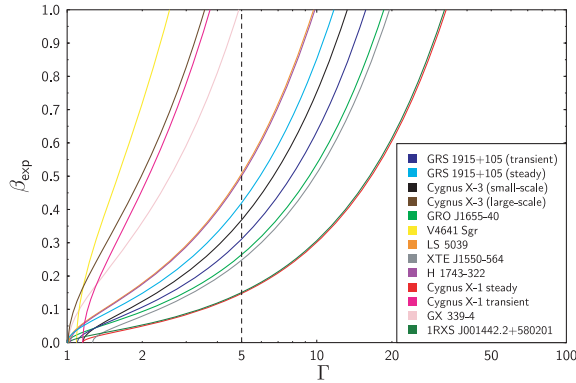

Figure 3. Predicted expansion speeds for measured Lorentz factors from equation (7) and the constraints on $\beta \cos i$ and ϕ given in Table 1. The vertical dashed line corresponds to a Lorentz factor of 5, showing that most jets must be confined ($\beta_{\mathrm{exp}} < 1$) if their observed opening angles are determined by the transverse Doppler effect.

3.4 Lorentz factors from source distances

By definition, all significantly relativistic jets should lie close to d_{max} (as defined in equation 6). Therefore, for sources at distances significantly less than d_{max}, we can constrain their Lorentz factors via

$$\Gamma = \left\{ 1 - \left(\frac{d}{d_{\mathrm{max}}} \right)^2 [1 - (\beta \cos i)^2] - (\beta \cos i)^2 \right\}^{-1/2}. \quad (10)$$

The derived values, Γ_{d}, are listed in Table 1 for the four sources with measured proper motions (such that d_{max} could be calculated)

and independently determined source distances. Since Γ increases rapidly as d approaches d_{max}, we can only put a lower limit on the Lorentz factors of the two sources lying close to (within 2σ of) d_{max}, GRS 1915+105 and GRO J1655−40. On the other hand, Cygnus X-3 and XTE J1550−564 both appear to lie at $d < d_{\mathrm{max}}$, so neither would appear to have a significantly relativistic jet.

3.5 Jets known to be confined

Further evidence for the jets in Cygnus X-3 and XTE J1550−564 being confined comes from the observed deceleration of the jets. In the milliarcsecond scale jets of Cygnus X-3 (Mioduszewski et al. 2001; Miller-Jones et al. 2004), the southern jet was found to be approaching and the northern counterjet receding from us. On arcsecond scales, however, the northern component is both brighter and at a greater angular separation than the southern component (Martí, Paredes & Peracaula 2001), suggesting that the southern component has decelerated on moving outwards. It must therefore have a low bulk Lorentz factor, $\lesssim 2$, on arcsecond scales at least. The distance discrepancy addressed in Section 3.4 suggests that the bulk Lorentz factor is also low on milliarcsecond scales. The X-ray jets of XTE J1550−564 showed a measurable decrease in the rate of angular separation from the core with time (Kaaret et al. 2003). In order to produce a measurable deceleration in the proper motions, the bulk Lorentz factor of the component must be $\lesssim 2$, since significant changes in proper motions for a (presumably) fixed angle to the line of sight are only possible when β is changing appreciably, i.e. in the regime $\Gamma \lesssim 2$. It is possible that the X-ray jets detected in H 1743−322 were also similarly powered by bulk deceleration, although the observations cannot confirm this. For Cygnus X-3 and

Table 2. Measured parameters needed to calculate jet power P_{min} from minimum energy arguments. Data taken mainly from Fender et al. (2004a). The Lorentz factors derived from opening angle considerations are not ruled out by jet power constraints except in the case of Cygnus X-3.

System	d (kpc)	$M/M_\odot$	Δt (s)	$S_{5\,GHz}$ (mJy)	$\beta \cos i$	P_{min}/L_{Edd}	$\Gamma_{min,exp}$
GRS 1915+105 (2001 transient)	11	14	21000	100	0.29 ± 0.09	0.03	3.3
GRS 1915+105 (1997 transient)	11	14	43200	320	0.41 ± 0.02	1.87	15.7
GRS 1915+105 (steady)	11	14	300	50	0.035 ± 0.017	0.09	11.7
Cygnus X-3 (small scale)	10	$\sim 4?$	3×10^5	13400	0.50 ± 0.10	43.3	13.3
GRO J1655 − 40	3.5	7	43200	2000	0.091 ± 0.014	13.9	18.6
V4641 Sgr	8	9	43200	420	~ 0.4	0.22	2.6
XTE J1550 − 564	6	9	43200	130	0.61 ± 0.13	1.92	19.6
Cygnus X-1 (steady)	2.5	10	2000	50	> 0.50	0.30	33.0
GX 339 − 4	8	7	19800	55	$> 0.16 \pm 0.05$	0.24	4.9

XTE J1550−564 therefore, since $\Gamma \lesssim 2$, Fig. 3 shows that the jets must be confined.

Although we have not plotted the Lorentz factor for SS 433 in Fig. 2, the jets in this source are certainly confined. The opening angles inferred from observations are $< 7°$ (Appendix A), whereas the predicted jet opening angle from equation (3) is at least $74°$ for transverse expansion at c, given the known bulk velocity of $0.26c$ (Abell & Margon 1979; Hjellming & Johnston 1981). Confinement (on small scales at least) was proposed for this source by Hjellming & Johnston (1988), who suggested that the jet underwent a transition from slowed to free expansion (i.e. became unconfined) at a distance of ~ 25 light days from the core. We know that the jets of SS 433 contain baryons, so it is possible that these cold protons could be responsible for the slowed expansion (see Section 6).

4 LOW/HARD STATE JETS

Two different manifestations of jets are known to exist in XRBs; steady, flat-spectrum outflows observed in the low/hard X-ray state (e.g. Dhawan, Mirabel & Rodríguez 2000b), and discrete superluminal ejecta seen during transient outbursts (e.g. Mirabel & Rodríguez 1994). According to the internal shock model of Fender et al. (2004a), the Lorentz factors of the steady jets should be lower than for the transient jets. Our sample contains both steady and transient jets in Cygnus X-1 and GRS 1915+105, so we can compare the derived Lorentz factors to see if there is a difference.

Steady jets are unlikely to be able to exceed the Eddington limit, a condition satisfied by the values of P_{min}/L_{Edd} given in Table 2. Comparing the Lorentz factors derived from opening angle considerations, $\Gamma_{min,exp}$ (listed in Table 1), for the transient and steady jets, there is no obvious trend. $\Gamma_{min,exp}$ for the steady jet in GRS 1915+105 is greater than that derived for the 2001 flare, but less than that for the 1997 flare. However, since neither in Cygnus X-1 nor in GRS 1915+105 were the jets resolved, the opening angles we have listed are all upper limits, and thus we would not necessarily expect to see a significant difference between the steady and the transient jets.

We cannot constrain the steady jets to be less relativistic than the transient jets from their opening angles. Therefore, if they are indeed significantly less relativistic, as predicted by the internal shock model, then the steady jets would have to be confined.

5 COMPARISON TO AGN

XRB jets are in general thought to be less relativistic than those in AGN. Their typical bulk Lorentz factors are commonly assumed to
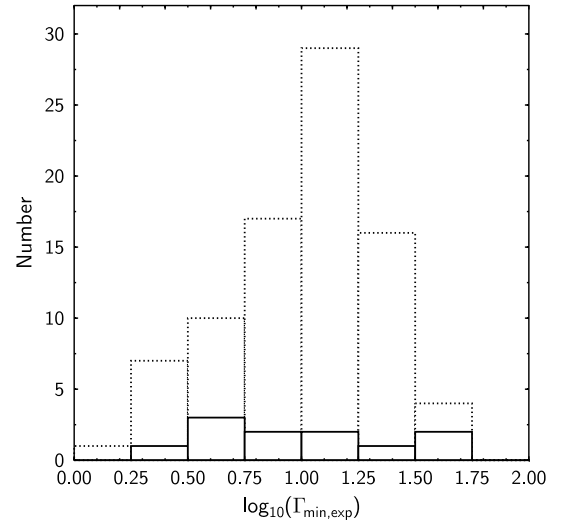

Figure 4. Distributions of Lorentz factors derived for XRB jets and AGN jets. The solid bars show the distribution for X-ray binary jets, assuming that they all have the minimum Lorentz factor permitted from opening angle considerations, and assuming free jet expansion. The dashed bars show the distribution for AGN jets, calculated using the proper motions tabulated by Jorstad et al. (2001), assuming that they all have the minimum permitted bulk Lorentz factors, with $\beta = \cos i$.

be of order 2–5, as compared to the AGN jets with bulk Lorentz factors up to ~ 20. A recent discovery of an ultrarelativistic outflow at $\beta_{app} > 15$ in Circinus X-1 (Fender et al. 2004b), later revised down to $\beta_{app} > 9.2$ by Iaria et al. (2005), challenges the assumption that stellar-mass objects cannot produce highly relativistic jets. From equation (2), the apparent component velocity β_{app} has a minimum value of $\Gamma\beta$ when $\beta = \cos i$, where β is the true component velocity. β_{app} is thus a lower limit to the value of Γ. Hence XRBs are clearly capable of producing jets with Lorentz factors ~ 10.

Proper motions for jet components in a sample of γ-ray bright blazars were measured by Jorstad et al. (2001). Fig. 4 shows the minimum bulk Lorentz factors derived from their tabulated values of β_{app} compared to those derived from the opening angle constraints for XRB jets in Section 3.2. The Lorentz factors for jets found to be confined in Section 3.5 have been omitted from the histogram. Since the sample is so small for the X-ray binaries, and since in both cases we have plotted lower limits on the Lorentz factors, a quantitative comparison is not possible. However, the histograms do show that *if* XRB jets are unconfined, and the derived opening angles are purely

due to the relativistic effect described in Section 2, then XRB jets can be at least as relativistic as AGN jets.

5.1 High-mass X-ray binaries

While Circinus X-1 is known to produce jets with high bulk Lorentz factors, no high-mass XRB is known to produce highly relativistic jets able to move ballistically outwards at $\beta \sim 1$ with no deceleration. We have already discussed the cases of SS 433 and Cygnus X-3. The transient jets of Cygnus X-1 were thought to have velocities $v \gtrsim 0.3c$, estimated from an assumed ejection date (Fender et al. 2006). In CI Cam, no jet was seen during the 1998 outburst, but rather an expanding radio nebula, consistent with a shock moving through a dense stellar wind (Mioduszewski & Rupen 2004). We therefore suggest that it is only the low-mass XRBs that can produce resolved jets with the high bulk Lorentz factors discussed herein, as a result of the more tenuous ambient medium. This does not mean that the high-mass XRBs are not launched with comparable Lorentz factors, but rather that their stronger interactions with the surrounding interstellar medium (ISM) tend to decelerate the jets before they become resolved.

6 CONFINEMENT MECHANISMS

Both Begelman, Blandford & Rees (1984) and Ferrari (1998) give detailed discussions on possible jet confinement mechanisms. The most natural confining agent for a jet is thermal gas pressure from an external medium or a magnetic field. The internal jet pressure, p_{min}, can be calculated from equipartition arguments, since

$$p_{min} = (\gamma_{SH} - 1)U_{min} = (\gamma_{SH} - 1)\frac{E_{min}}{V}, \qquad (11)$$

where U_{min} is the minimum energy density in the source, and γ_{SH} is the ratio of specific heats, equal to 4/3 for an ultrarelativistic gas. A minimum energy density can be found by dividing the minimum energy E_{min} corresponding to the observed synchrotron emission by the source volume, V. If the pressure of the external medium is given by the ideal gas law, $p = nk_B T$, where k_B is Boltzmann's constant, n the number density of particles and T the temperature, then typical ISM number densities and temperatures give pressures several orders of magnitude too low to confine the jets. This is unsurprising, since Heinz (2002) found that microquasars inhabit low-density, low-pressure environments when compared in a dynamical sense to the environments of AGN. We do not therefore consider pressure confinement by the ambient ISM to be a possibility.

One of the major differences between microquasars and AGN is that AGN jets tend to be surrounded by observable cocoons of waste plasma flowing back from the hotspots at the ends of the jets. This plasma is at higher pressure than the ambient ISM, helping to confine the jet. Such cocoons have only been detected in a few Galactic systems. Cygnus X-1 is known to have inflated a bubble in the ISM, whose bow shock has been imaged (Gallo et al. 2005), although the surface brightness of the lobes themselves was too low to be detected. The jets in SS 433 have deformed the supernova remnant W 50, creating a pair of lateral extensions with position angles in perfect agreement with the jet axis (e.g. Dubner et al. 1998). Possible hotspot-like structures have recently been tentatively associated with the sources GRS 1915+105 (Rodríguez & Mirabel 1998; Chaty et al. 2001; Kaiser et al. 2004) and Cygnus X-3 (Martí et al. 2005), although any association with the source is yet to be definitively confirmed in either case. Lobe structures have, as stated in Appendix A, been detected in the sources 1E 1740.7−2942 and GRS 1758−258,

but in neither source have the jets themselves been observed. Heinz (2002) found that since microquasar sources stay relativistic for a dynamically longer time than AGN, and are located in underdense environments, their detectability will be severely limited and only possible at low frequencies. Such low-frequency observations with new and upcoming facilities such as the new Low Frequency Front Ends on the Westerbork Synthesis Radio Telescope, and the Low Frequency Array (LOFAR; Röttgering et al. 2003) may shed light on this issue.

Icke et al. (1992) suggested that jets could be inertially confined (on small scales at least) by an outflowing wind around the jet, whose ram pressure would oppose the jet expansion. Peter & Eichler (1995) investigated inertial confinement, and found that inertial effects could collimate a jet provided that the material to be collimated was sufficiently tenuous compared to the surrounding flow responsible for the collimation.

A toroidal magnetic field can, in theory, confine a jet via the hoop stress mechanism, although toroidal fields are notoriously unstable to the kink instability, which could disrupt the jet. Furthermore, Eichler (1993) found that magnetically confined jets are subject to only a modest amount of collimation in the absence of an additional collimating mechanism. So far from the anchor point of the magnetic field, some dynamo effect would likely be required to maintain a sufficiently strong magnetic field. However, Spruit, Foglizzo & Stehle (1997) suggested that poloidal fields could lead to collimation at some collimation distance of order the disc radius, after which the jet would remain collimated, expanding ballistically with a fixed opening angle out to large distances. If the jet material was simply streaming ballistically outwards, no collimating mechanism would be required.

A final possibility is that the jet could contain cold material; either protons or pairs. Since we observe synchrotron radiation in the radio band, we know that there are highly relativistic electrons present in the jets. This could just be the high-energy tail of a thermal population of pairs, although we consider this unlikely given the observed relativistic bulk velocities. However, if cold protons (non-relativistic in the comoving frame) were present, they would dominate the inertia of the jets unless the mean electron Lorentz factors were $\gtrsim 2000$. Applying minimum energy arguments to the X-ray emitting knots in XTE J1550−564 (Tomsick et al. 2003) gives a mean electron Lorentz factor of $7.8 \times 10^3 < \langle \gamma_e \rangle < 2.9 \times 10^4$, depending on the source distance. In this case, assuming equipartition of energy between protons and electrons, even the protons would have $\langle \gamma_p \rangle > 4.25$. So cold protons do not in all cases dominate the inertia of XRB jets, but if they were to do so, the expansion would be retarded compared to a plasma consisting solely of electron–positron pairs. This confinement mechanism has been effectively ruled out in AGN by Celotti et al. (1998), who found that the filling factor of the jet with thermal material had to be so small as to be insignificant in terms of the overall jet energy budget. As mentioned in Section 3.5, this mechanism could be responsible for confinement in SS 433.

6.1 Light curves: a possible test of confinement

A possible test of whether the jets are confined could be made using jet light curves. The magnetic field in the jet scales as $V^{-2/3}$ for a non-turbulent jet, where V is the jet volume. The Lorentz factor of the particles in an adiabatically expanding jet scales as $V^{-1/3}$, and thus the jet emissivity scales as $J \propto V^{(4\alpha-2)/3}$. For a jet expanding freely at constant velocity, $V \propto t^3$, so the flux density scales as $S \propto t^{(4\alpha-2)}$. The magnetic field would fall off more slowly with jet volume for a turbulent jet (typically as $V^{(-2+\zeta)/3}$, where $\zeta \sim 1$

describes the degree of turbulence). We note however that once the magnetic field energy has reached equipartition with the internal energy, a decay slower than $B \propto V^{-1/2}$ is not possible on energetics grounds. Fitting the jet light curves in the optically thin part of the spectrum with a power-law decay, $S = S_0(t/t_0)^{-\xi}$, we can then place limits on the confinement of the jets. For a typical optically thin jet, $\alpha \sim -0.6$, and since the power-law index ξ is Lorentz invariant, we would expect $\xi \sim 4$ if the jets are freely expanding (the exact value depending on the degree of turbulence). If ξ is much less than this ($\lesssim 3$), the jets are not expanding at constant velocity, which strongly indicates jet confinement, as there is no reason that the volume of a confined jet would scale as t^3.

To measure the flux density decay with time, the jet light curve must be decoupled from that of the core, which requires both resolving the jets, and measuring their flux density at more than two epochs. Nevertheless, Rodríguez & Mirabel (1999) measured power-law indices of 1.3 ± 0.2 close to the core and 2.6 ± 0.5 at distances $> 2 \times 10^{17}$ cm in GRS 1915+105, suggesting a switch from confined to free expansion (as previously suggested for SS 433). Miller-Jones et al. (2005) measured 1.80 ± 0.03 and 2.01 ± 0.02 in the same source for two outbursts in 2001 on scales smaller still, confirming the confinement at small angular separations. The X-ray flux in XTE J1550−564, on the other hand, was observed to decay with a power-law index of 3.7 ± 0.7 (Kaaret et al. 2003), so the X-ray jets in this source could be expanding at constant velocity. Since we found in Section 3.5 that the jets in this source are almost certainly confined, the expansion velocity is likely to be less than c, if constant.

In summary, we cannot easily rule out many of the possible confinement mechanisms in XRB jets, and the evidence from the decay light curves of the two sources considered above suggests that the jets are not freely expanding. Should the jets be confined, they would not need to be as relativistic as implied by the opening angle calculations of Section 3.2. But given the differences in conditions between the environments of Galactic and extragalactic objects outlined in this section, and the likely variations in those properties within the Galaxy, it is at least plausible that XRB jets need not all be confined.

7 CONCLUSIONS

If XRB jets are not confined, but are expanding freely, it is possible to constrain their Lorentz factors from measurements of the jet opening angles. The small opening angles we observe are in this case a consequence of the transverse Doppler effect slowing the apparent expansion speed in the observer's frame. From the upper limits to the opening angles quoted in the literature, the Lorentz factors thus derived are significantly more relativistic (with a mean Lorentz factor > 10) than is commonly assumed, and possibly no less so than AGN jets. However, if the jets we observe do indeed have Lorentz factors in the commonly assumed range of 2–5, then we can quantify the degree of confinement. The lateral expansion speed perpendicular to the jet axis must then in some cases be $\lesssim 0.15c$.

In most cases, we cannot exclude the possibility that the jets are unconfined from jet power constraints, nor from measurements of the proper motions of knots in XRB jets. From the distances $d \ll d_{\mathrm{max}}$ and the observed deceleration in the jets of Cygnus X-3 and XTE J1550−564, we know that the jets in these sources at least must be confined. The observed opening angle of the jets in SS 433 suggests that its jets are also confined, possibly by the cold protons known to exist in the jets. However, we cannot definitively rule out confinement in any of the other sources considered. We do not find any evidence for a difference in the velocities of low/hard state jets and transient jets, although the observations only provided lower limits to the Lorentz factors in both cases.

In many cases, and as observed in Circinus X-1, XRB jets could well be significantly more relativistic than is commonly assumed, although this is unlikely in the case of high-mass XRBs. While we cannot rule out many of the possible confinement mechanisms, in the absence of definitive lower limits to the jet Lorentz factors, the possibility that XRB jets are highly relativistic ($\Gamma \sim 10$) should not be ruled out.

REFERENCES

Abell G. O., Margon B., 1979, Nat, 279, 701
Begelman M. C., Hatchett S. P., McKee C. F., Sarazin C. L., Arons J., 1980, ApJ, 238, 722
Begelman M. C., Blandford R. D., Rees M. J., 1984, Rev. Mod. Phys., 56, 255
Celotti A., Kuncic Z., Rees M. J., Wardle J. F. C., 1998, MNRAS, 293, 288
Chaty S., Rodríguez L. F., Mirabel I. F., Geballe T. R., Fuchs Y., Claret A., Cesarsky C. J., Cesarsky D., 2001, A&A, 366, 1035
Corbel S., Fender R. P., Tzioumis A. K., Tomsick J. A., Orosz J. A., Miller J. M., Wijnands R., Kaaret P., 2002, Sci, 298, 196
Corbel S., Kaaret P., Fender R. P., Tzioumis A. K., Tomsick J. A., Orosz J. A., 2005, ApJ, 632, 504
Dhawan V., Goss W. M., Rodríguez L. F., 2000a, ApJ, 540, 863
Dhawan V., Mirabel I. F., Rodríguez L. F., 2000b, ApJ, 543, 373
Dickey J. M., 1983, ApJ, 273, L71
Dubner G. M., Holdaway M., Goss W. M., Mirabel I. F., 1998, AJ, 116, 1842
Eichler D., 1993, ApJ, 419, 111
Fender R. P., 2003, MNRAS, 340, 1353
Fender R. P., Garrington S. T., McKay D. J., Muxlow T. W. B., Pooley G. G., Spencer R. E., Stirling A. M., Waltman E. B., 1999, MNRAS, 304, 865
Fender R. P., Belloni T. M., Gallo E., 2004a, MNRAS, 355, 1105
Fender R. P., Wu K., Johnston H., Tzioumis A. K., Jonker P. G., Spencer R. E., van der Klis M., 2004b, Nat, 427, 222
Fender R. P., Stirling A. M., Spencer R. E., Brown I., Pooley G. G., Muxlow T. W. B., Miller-Jones J. C. A., MNRAS, in press (doi:10.1111/j.1365-2966.2006.10193.x) (astro-ph/0602307)
Ferrari A., 1998, ARA&A, 36, 539
Fomalont E. B., Geldzahler B. J., Bradshaw C. F., 2001, ApJ, 558, 283
Fuchs Y. et al., 2003, A&A, 409, L35
Gallo E., Fender R. P., Pooley G. G., 2003, MNRAS, 344, 60
Gallo E., Corbel S., Fender R. P., Maccarone T. J., Tzioumis A. K., 2004, MNRAS, 347, L52
Gallo E., Fender R., Kaiser C., Russell D., Morganti R., Oosterloo T., Heinz S., 2005, Nat, 436, 819
Heinz S., 2002, A&A, 388, L40
Heinz S., Merloni A., 2004, MNRAS, 355, L1
Hjellming R. M., Johnston K. J., 1981, ApJ, 246, L141
Hjellming R. M., Johnston K. J., 1988, ApJ, 328, 600
Hjellming R. M., Rupen M. P., 1995, Nat, 375, 464
Hjellming R. M. et al., 2000, ApJ, 544, 977
Hynes R. I., Steeghs D., Casares J., Charles P. A., O'Brien K., 2004, ApJ, 609, 317
Iaria R., Spanò M., Di Salvo T., Robba N. R., Burderi L., Fender R., van der Klis M., Frontera F., 2005, ApJ, 619, 503
Icke V., Mellema G., Balick B., Eulderink F., Frank A., 1992, Nat, 355, 524

Jorstad S. G., Marscher A. P., Mattox J. R., Wehrle A. E., Bloom S. D., Yurchenko A. V., 2001, ApJS, 134, 181

Kaaret P., Corbel S., Tomsick J. A., Fender R. P., Miller J. M., Orosz J. A., Tzioumis A. K., Wijnands R., 2003, ApJ, 582, 945

Kaiser C. R., Gunn K. F., Brocksopp C., Sokoloski J. L., 2004, ApJ, 612, 332

Landau L. D., Lifshitz E. M., 1959, Course of Theoretical Physics, Vol. 6: Fluid Mechanics, 2nd edn. Elsevier Butterworth-Heinemann, Oxford, p. 318

Longair M. S., 1994, High Energy Astrophysics, Vol. 2: Stars, the Galaxy and the Interstellar Medium, 2nd edn. Cambridge Univ. Press, Cambridge.

Maccarone T. J., 2003, A&A, 409, 697

Marshall H. L., Canizares C. R., Schulz N. S., 2002, ApJ, 564, 941

Martí J., Paredes J. M., Peracaula M., 2001, A&A, 375, 476

Martí J., Mirabel I. F., Rodríguez L. F., Smith I. A., 2002, A&A, 386, 571

Martí J., Pérez-Ramírez D., Garrido J. L., Luque-Escamilla P., Paredes J. M., 2005, A&A, 439, 279

Massey P., Johnson K. E., Degioia-Eastwood K., 1995, ApJ, 454, 151

Miller-Jones J. C. A., Blundell K. M., Rupen M. P., Mioduszewski A. J., Duffy P., Beasley A. J., 2004, ApJ, 600, 368

Miller-Jones J. C. A., McCormick D. G., Fender R. P., Spencer R. E., Muxlow T. W. B., Pooley G. G., 2005, MNRAS, 363, 867

Mioduszewski A. J., Rupen M. P., 2004, ApJ, 615, 432

Mioduszewski A. J., Rupen M. P., Hjellming R. M., Pooley G. G., Waltman E. B., 2001, ApJ, 553, 766

Mirabel I. F., Rodríguez L. F., 1994, Nat, 371, 46

Mirabel I. F., Rodríguez L. F., Cordier B., Paul J., Lebrun F., 1992, Nat, 358, 215

Orosz J. A. et al., 2001, ApJ, 555, 489

Orosz J. A. et al., 2002, ApJ, 568, 845

Paredes J. M., Ribó M., Ros E., Martí J., Massi M., 2002a, A&A, 393, L99

Paredes J. M., Ribó M., Martí J., 2002b, A&A, 394, 193

Peter W., Eichler D., 1995, ApJ, 438, 244

Ribó M., Paredes J. M., Romero G. E., Benaglia P., Martí J., Fors O., García-Sánchez J., 2002a, A&A, 384, 954

Ribó M., Ros E., Paredes J. M., Massi M., Martí J., 2002b, A&A, 394, 983

Ribó M., Dhawan V., Mirabel I. F., 2004, in Bachiller R., Colomer F., Desmurs J. F., de Vicente P., eds, Proc. 7th Symp. the European VLBI Network on New Developments in VLBI Science and Technology. Observatorio Astronomico Nacional of Spain, Toledo, p. 111

Rodríguez L. F., Mirabel I. F., 1998, A&A, 340, L47

Rodríguez L. F., Mirabel I. F., 1999, ApJ, 511, 398

Rodríguez L. F., Mirabel I. F., Martí J., 1992, ApJ, 401, L15

Röttgering H., de Bruyn A. G., Fender R. P., Kuijpers J., van Haarlem M. P., Johnston-Hollitt M., Miley G. K., 2003, in Bandiera R., Maiolino R., Mannucci F., eds, XXI Symp. Relativistic Astrophysics: Texas in Tuscany. World Scientific Press, Singapore, p. 69

Sari R., Piran T., Halpern J. P., 1999, ApJ, 519, L17

Shahbaz T., Fender R. P., Charles P. A., 2001, A&A, 376, L17

Spruit H. C., Foglizzo T., Stehle R., 1997, MNRAS, 288, 333

Stirling A. M., Spencer R. E., de la Force C. J., Garrett M. A., Fender R. P., Ogley R. N., 2001, MNRAS, 327, 1273

Tomsick J. A., Corbel S., Fender R. P., Miller J. M., Orosz J. A., Tzioumis A. K., Wijnands R., Kaaret P., 2003, ApJ, 582, 933

Vermeulen R. C., Schilizzi R. T., Spencer R. E., Romney J. D., Fejes I., 1993, A&A, 270, 177

Zdziarski A. A., Poutanen J., Mikolajewska J., Gierlinski M., Ebisawa K., Johnson W. N., 1998, MNRAS, 301, 435

APPENDIX A: THE INDIVIDUAL SOURCES

Here we present a summary of the observations on the individual X-ray binaries which have been observed to exhibit resolved jets.

GRS 1915+105: Discrete knots in this system have been followed as they moved outwards from the core (Mirabel & Rodríguez 1994; Fender et al. 1999; Miller-Jones et al. 2005). We chose the highest resolution observations (Fender et al. 1999) to constrain $\beta \cos i =$ 0.41 ± 0.02. From the lack of resolved structure perpendicular to the jet axis, the half-opening angle is constrained to be $\leqslant 4°$. Milliarcsecond scale radio jets have also been imaged during the X-ray hard plateau state in this source (Dhawan et al. 2000b; Fuchs et al. 2003; Ribó, Dhawan & Mirabel 2004). Dhawan et al. found that these jets were marginally resolved perpendicular to the jet axis at 43 GHz, although in this case the opening angle cannot be derived as the black hole position is not known (V. Dhawan, private communication). From the beam size and jet length in their lower-resolution 15-GHz images, we derived a constraint on the half-opening angle of $\leqslant 5°$.

Cygnus X-3: Again, discrete knots have been followed as they moved out from the core of the system (Miller-Jones et al. 2004). The ratio of proper motions of approaching and receding jet components constrained $\beta \cos i = 0.50 \pm 0.10$, and the measured knot size perpendicular to the jet axis from the last high-resolution 22-GHz image was used to constrain the half-opening angle to be $5.0 \pm 0.5°$. On larger scales, Martí et al. (2001) found $\beta \cos i > 0.14 \pm 0.03$ and did not resolve the knots perpendicular to the jet axis at an angular separation of ∼0.6 arcsec with a beam diameter of 361 mas, giving an upper limit on the half-opening angle of $\phi < 16.5°$.

GRO J1655−40: The highest resolution observations of the 1994 outburst of GRO J1655−40 were made by Hjellming & Rupen (1995) at 1.6 GHz with the Very Long Baseline Array (VLBA). The ejecta were observed moving out to a maximum separation of ∼1 arcsec, and the beamwidth was ∼43 × 108 mas, with no evidence for the jets being resolved. This constrained the opening angle to $\leqslant 6.1°$. From the ratio of proper motions of the north-west and south-east ejecta, $\beta \cos i = 0.091 \pm 0.014$, and the kinematic model gives a distance of 3.2 ± 0.2 kpc.

V4641 Sgr: Hjellming et al. (2000) observed the 1999 September outburst of V4641 Sgr at 4.9 GHz with the Very Large Array (VLA), and found an extended jet-like structure at an angular separation of 0.25 arcsec. The restoring beam was a circular Gaussian of full width at half-maximum (FWHM) 0.3 arcsec, constraining the opening angle to be $\leqslant 50.2°$. From the kink in the light curve of the outburst, attributed to the offset between the peaks in the approaching and receding jets, they found $\beta \cos i = 0.4$. They argued that the source distance lies in the range $0.4 \leqslant d \leqslant 1.7$ kpc with the nearer distance being most likely, in stark contradiction to the distance of $9.59^{+2.72}_{-2.19}$ kpc found from the luminosity of the secondary star (Orosz et al. 2001).

LS 5039: A two-sided milliarcsecond scale radio jet in LS 5039 was observed at 5 GHz with the European VLBI Network (EVN) and Multi-Element Radio-Linked Interferometer Network (MERLIN) (Paredes et al. 2002a). Using the length asymmetry of the jets on either side of the core, $\beta \cos i = 0.17 \pm 0.05$ and since the jet width was smaller than one synthesized beam, the half-opening angle was constrained to $\leqslant 6°$.

XTE J1550−564: Corbel et al. (2002) first detected radio and X-ray emitting jets from XTE J1550−564, which they found to be decelerating with time. Tomsick et al. (2003) found no evidence for extension perpendicular to the jet axis in the approaching (eastern) jet, constraining the opening angle to be $<7.5°$ at an angular separation of 23.4 ± 0.5 arcsec. In observations taken 2 yr later, Kaaret et al. (2003) found weak evidence for extension perpendicular to the jet axis in the receding (western) X-ray jet at a similar angular separation, giving a more stringent limit on the half opening angle of $<1°$. From the measured proper motions of the eastern and western jets, assuming symmetric jet propagation, they found $\beta \cos i = 0.61 \pm 0.13$ and $d_{max} = 16.5 \pm 3.5$ kpc. The true distance was found to be in the range $1.4 < d < 9.8$ kpc from the observed luminosity of the

secondary star, and $3.2 < d < 10.8$ kpc from the systemic velocity, with a favoured value of 5.3 kpc (Orosz et al. 2002). For consistency with other sources, we will use the half-opening angle constraint of Tomsick et al. (2003), since it is measured for the approaching jet.

H 1743−322: Corbel et al. (2005) detected moving X-ray jets from another microquasar system, H 1743−322. Assuming ballistic jet motion, they found $\beta \cos i = 0.23 \pm 0.05$ and $d_{max} = 10.4 \pm 2.9$ kpc. The upper limit on the source FWHM was found to be 1.4 arcsec at an angular separation of 6.63 arcsec, implying an opening angle of $<12°$. The source lies in the direction of the Galactic Centre, so its distance was assumed to be 8.5 kpc, although no definitive measurement has yet been made.

Cygnus X-1: Stirling et al. (2001) imaged an extended jet-like radio structure in Cygnus X-1 while the source was in the low/hard X-ray state. The jet was not resolved perpendicular to the flow, constraining the half-opening angle to be $\leqslant 2°$. From the ratio of the flux density in the detected jet to the upper limit on the flux density in the receding jet (the rms noise in the image multiplied by the area occupied by the approaching jet), a value for $\beta \cos i$ may be obtained from the equation

$$\frac{S_{app}}{S_{rec}} = \left(\frac{1 + \beta \cos i}{1 - \beta \cos i} \right)^{k-\alpha}, \tag{A1}$$

where $k = 2$ for a continuous jet and $k = 3$ for a jet composed of discrete knots. Taking $k = 3$ and a spectral index $\alpha = -0.6$ gives the minimum likely value $\beta \cos i > 0.5$. More recently, Fender et al. (2006) have detected a resolved transient jet from this source at an angular separation of 70 ± 5 mas, unresolved with a beam size of 50 mas, implying an opening angle of $36°$. The bulk jet velocity was found to be $\gtrsim 0.3c$, which, if the jet and disc are aligned ($i = 30°$), implies $\beta \cos i > 0.2$.

GX 339−4: After an outburst in 2002 May, Gallo et al. (2004) detected variable extended structure in GX 339−4. At the latest epoch, the knot was separated from the core by 6.9 arcsec with a beamwidth of 3.06 arcsec, implying an opening angle of $\leqslant 24°$. From equation (A1) and the known spectral index of -0.98 ± 0.10 gives a constraint $\beta \cos i \geqslant 0.56$. The source distance is an issue of considerable debate. Systemic velocity measurements gave 4 ± 1 kpc (Zdziarski et al. 1998), whereas the upper limit on the magnitude of the secondary star implies $d > 5.6$ kpc (Shahbaz, Fender & Charles 2001). Maccarone (2003) estimated $d > 7.6$ kpc from the X-ray state transition luminosity, and interstellar absorption mea-

surements suggest a distance of at least 6 kpc, and possibly as high as 15 kpc (Hynes et al. 2004). The distance should therefore be considered highly uncertain.

1RXS J001442.2+580201: Identified as a microquasar candidate by Paredes, Ribó & Martí (2002b), resolved jets were detected in this source by Ribó et al. (2002b). The latter also found a 3σ result for detectable source proper motion suggestive of a Galactic nature, for which reason this source is included in our sample. From the angular separations of the components from the core, they found $\beta \cos i = 0.20 \pm 0.02$. The components were unresolved with the EVN beam of 0.86 mas, giving a constraint on the opening angle of $<3.6°$. With no detected component proper motions, no constraint can be placed on d_{max}.

SS 433: The most stringent (albeit model dependent) limits on the opening angle of the jet in SS 433 come from the widths of X-ray lines measured by Marshall, Canizares & Schulz (2002), ascribed to the Doppler broadening due to a conical outflow of constant opening angle. The half opening angle of the jet was found to be $0.61 \pm 0.03°$, which may be compared to the upper limit of $6.8°$ found from radio observations (Vermeulen et al. 1993), and to that of $\lesssim 5°$ found from the widths of the optical emission lines (Begelman et al. 1980). The jet velocity is known to be $\beta = 0.26 \pm 0.05$ and the inclination angle of the jet axis to the line of sight is $80°$ (Hjellming & Johnston 1981), although since the jet precesses, the inclination angle to the line of sight changes, so we have not included this source in our calculations.

The two confirmed neutron stars with resolved jets, Scorpius X-1 (Fomalont, Geldzahler & Bradshaw 2001) and Circinus X-1 (Fender et al. 2004b) have not been included in this survey, since it seems that the lobes we see are the working surface where an ultrarelativistic, unseen flow of energy impacts on the ambient medium. It is therefore not possible to constrain the opening angle of the jet from the sizes of the lobes. Also, radio lobes have been detected in the black hole candidates 1E 1740.7−2942 (Mirabel et al. 1992) and GRS 1758−258 (Rodríguez, Mirabel & Martí 1992; Martí et al. 2002), but the lack of proper motion in both sources again argues for these lobes being hotspots where the jets impact the ISM, so they cannot be used to constrain the jet opening angles.

This paper has been typeset from a TEX/LATEX file prepared by the author.